

Single-Crystal Metal–Organic Framework Arrays

Carlos Carbonell, Inhar Imaz, and Daniel Maspoch*

CIN2(ICN-CSIC), Catalan Institute of Nanotechnology, Esfera UAB, 08193 Bellaterra, Spain

S Supporting Information

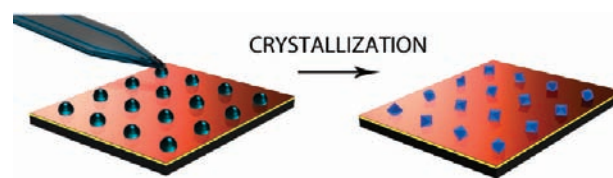
ABSTRACT: A novel, versatile pen-type lithography-based methodology was developed to control the growth of HKUST-1 crystals on surfaces by direct delivery of femtoliter droplets containing both inorganic and organic building block precursors. This approach shows that through the use of surfaces with low wettability it is possible to control the crystallization of a single submicrometer metal–organic framework crystal at a desired location on a surface.

Metal–organic frameworks (MOFs) represent an emerging class of crystalline inorganic–organic hybrid materials that are receiving considerable attention because they offer a wide range of potential applications, such as gas storage, catalysis, separation, sensing, and drug delivery.¹ Depending upon the intended application, one wants to be able to fabricate such frameworks as bulk crystalline solids, miniaturize them at the micro- or nanometer scale,² or control their deposition on surfaces.³ In the last case, the control of their growth, orientation, and/or positioning on the surface will be crucial in starting to conceive the integration of these MOFs on supports for the fabrication of complex surface sensors, separation membranes, drug-delivery platforms, and catalysts.⁴ In fact, the patterning of other functional materials, such as nanoparticles, organic polymers, biological entities, etc., has expanded their applications in a wide range of areas from microelectronics to optics, microanalysis to sensors, and magnetic systems to cell biology.⁵

Previous studies have shown that MOFs such as MOF-5,⁶ HKUST-1,⁷ MOF-508,⁸ and ZIF-7⁹ can be grown as crystalline thin films on surfaces by first functionalizing them with self-assembled monolayers (SAMs) or using presynthesized seeds. With the use of SAMs, Fischer and co-workers further demonstrated that MOF-5 crystals could be selectively grown on $40\ \mu\text{m} \times 40\ \mu\text{m}$ COOH-terminated SAM features fabricated by micro-contact printing.⁶ More recently, Wöll and co-workers¹⁰ used these COOH-terminated SAM templates to grow layer-by-layer HKUST-1 crystals, whereas De Vos and co-workers¹¹ controlled their growth on specific locations of a surface using the lithographically controlled wetting technique. In this communication, we report a novel on-surface MOF growth strategy that uses a wet lithographic technique for direct delivery of femtoliter droplets containing both inorganic and organic building block precursors, which after their reaction and droplet evaporation allows the fabrication of arrays of submicrometer HKUST-1 crystals on alkanethiol-modified gold surfaces.

Pen-type lithography techniques, such as fluidic-enhanced molecular transfer operation (FEMTO),¹² dip-pen nanolithography

Scheme 1. Schematic Illustration of the Fabrication of Single-Crystal MOF Arrays by Using Direct-Write FEMTO



(DPN),¹³ and fountain-pen lithography (FPL),¹⁴ allow the transfer of desired substances onto surfaces at the micro- and nanometer length scale through a scanning probe microscopy (SPM) probe or cantilever that dispenses femtoliter droplets of a solution containing these species. Thus, one could imagine their use to deliver droplets of a solution containing the organic and inorganic building blocks needed to build up a desired MOF onto specific regions of a surface. Once these droplets were positioned on the surface, the formation and crystallization of MOFs could be confined within each deposited droplet by controlling its evaporation and/or using external conditions such as microwave radiation or high temperature (Scheme 1). Following this strategy, we show herein that the controlled delivery of droplets containing a solution of Cu(II) ions and trimesic acid (H_3btc) onto surface-modified gold substrates leads to the fabrication of arrays of HKUST-1¹⁵ single crystals. This versatile strategy allows us to control the miniaturization and positioning of HKUST-1 crystals even at the single-crystal level on supports, enabling the creation of any desired pattern in a given experiment without the need for prefabricated stamps.

In a typical experiment, the inking solution was obtained by mixing $\text{Cu}(\text{NO}_3)_2 \cdot 2.5\text{H}_2\text{O}$ (1.170 g) and H_3btc (0.580 g) in pure dimethyl sulfoxide (DMSO, 5 g). Next, a commercially available surface patterning tool (SPT, BioForce USA) that had been cleaned with plasma for 15 min (UV/Ozone Procleaner, BioForce, USA) was directly charged with this solution by the addition of a microdroplet of the filtered solution into the reservoir of the SPT with a micropipet. The tip was brought into contact with surfaces functionalized with SAMs made of 11-mercapto-1-undecanol (MUOL), 16-mercaptohexadecanoic acid (MHA), 1-aminoundecanethiol (AUT), 1-octadecanethiol (ODT), or 1*H*,1*H*,2*H*,2*H*-perfluorodecanethiol (PFDT) to fabricate arrays of droplets of this solution over the substrate. All of the patterning was done with an Enabler Bioforce System (BioForce USA) at room temperature using a minimum dwell time of

Received: January 10, 2011

Published: January 31, 2011

0.001 s. The fabricated arrays were then placed into ambient conditions for 24 h until the DMSO was completely evaporated to form HKUST-1 crystals, as confirmed by energy-dispersive X-ray spectroscopy (EDX; Figure S2 in the Supporting Information), X-ray diffraction (XRD), and scanning electron microscopy (SEM).

A series of SAM surfaces bearing different functionalities that vary the contact angle between the DMSO precursor solution and the surface (functionalities and measured contact angles: $-\text{OH}$, $<10^\circ$; $-\text{COOH}$, $17.6 \pm 2.35^\circ$; $-\text{NH}_2$, $28.9 \pm 2.40^\circ$; $-\text{CH}_3$, $83 \pm 0.33^\circ$; $-\text{CF}_3$, $100.7 \pm 0.29^\circ$) were systematically studied first to determine the behavior of the droplets placed on these surfaces. Under the conditions studied, CH_3 - and CF_3 -terminated SAMs proved to be ideal for the fabrication of well-defined droplet arrays, whereas these arrays could not be fabricated on the OH - and COOH -terminated SAMs. When a droplet was placed on a OH - or COOH -terminated SAM, it spread completely. In contrast, the same droplet left on a CH_3 - or CF_3 -terminated SAM remained stuck in its place. The contact angle was then critical for droplet array formation. At low contact angles, the droplets tended to spread out completely once they were placed on the surface because the affinity and wettability of the solution on the surface was very high, thus preventing the formation of droplet arrays. This behavior was observed for both MUOL and MHA SAMs. However, as the contact angle between the solution and the surface increased, the affinity and spread diameter of the droplets decreased. This tendency could be observed for the AUT SAM, in which the patterned droplets also tended to spread out partially but not completely, thus allowing their structuration with a spread diameter larger than for the ODT and PFDT SAMs.

The tendency of the droplets to remain more stuck on surfaces with low wettability was further proven by fabricating a droplet array on a surface modified with NH_2 - and CF_3 -terminated SAMs (Figure 1a). Initially, we used FEMTO to generate patterns of AUT consisting of nine dots with diameters of $10 \mu\text{m}$ spaced $40 \mu\text{m}$ apart on a gold substrate. The exposed gold regions of the substrate were passivated with PFDT. FEMTO was then used to fabricate a 9×9 array of droplets of the DMSO precursor solution spaced $10 \mu\text{m}$ apart onto the AUT dot array area. As shown in Figure 1b, the resulting array contained 81 droplets, of which nine matched up the NH_2 -terminated dots (as marked by the dashed circles in Figure 1b) and the others were directly patterned on the CF_3 -terminated SAM. The diameters of the droplets were estimated to be around 5 and $3 \mu\text{m}$ for the ones placed on the NH_2 - and CF_3 -terminated SAMs, respectively. The above results confirm that DMSO precursor droplets spread out more on the NH_2 -terminated SAMs than on the nonpolar CF_3 -terminated SAMs when patterned using identical conditions (dwell time = 0.001 s, humidity = 35%, room temperature).

HKUST-1 arrays were fabricated by exposure of the patterned droplet arrays on the SAM-modified gold substrates at room temperature for 24 h. Figure 1c shows field-emission SEM (FESEM) images of the HKUST-1 array resulting from the evaporation of the 9×9 DMSO precursor droplet array. Interestingly, well-shaped octahedral crystals of HKUST-1 were grown in the contact areas between all of the FEMTO-delivered droplets and the SAMs. However, all nine droplets placed on the NH_2 -terminated dots yielded multiple crystals with edge dimensions ranging from 300 to 750 nm, whereas the remaining droplets placed on the CF_3 -terminated SAM yielded single

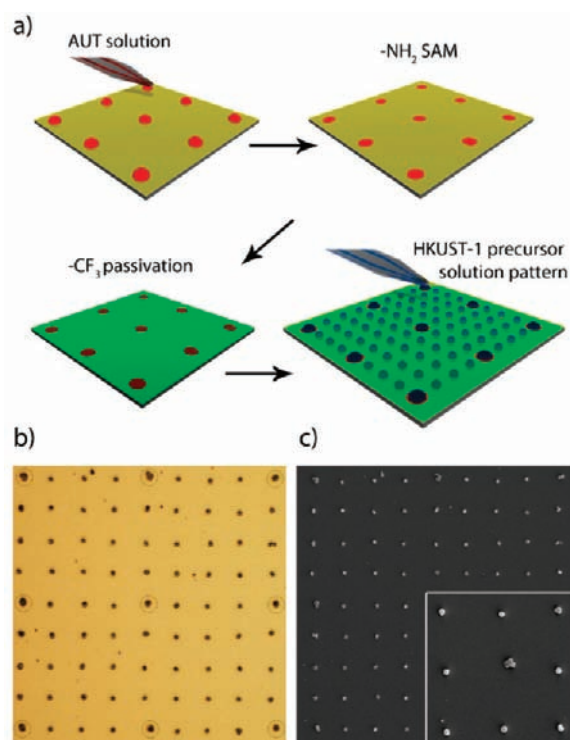


Figure 1. (a) Schematic illustration of the process followed for fabricating the 9×9 droplet array on a gold substrate previously patterned with a 3×3 AUT dot array and passivated with PFDT. (b) Optical microscopy image of the 9×9 droplet array, in which the droplets were spaced apart by $10 \mu\text{m}$. Dashed circles mark the nine droplets placed on AUT dots. (c) FESEM image of the resulting HKUST-1 array. The inset shows a magnified area of this array in which the central dot corresponds to multiple HKUST-1 crystals grown in a droplet placed on the AUT SAM and the other eight correspond to single HKUST-1 crystals grown in droplets placed on the PFDT SAM.

HKUST-1 crystals with edge dimensions between 800 nm and $1.2 \mu\text{m}$. The terminal group on the top of the SAMs, and therefore, the contact angle between the precursor droplet and the surface were again critical in determining the number and dimensions of the HKUST-1 crystals grown within each droplet, opening up the possibility of creating single-crystal HKUST-1 arrays on surfaces with low wettability. For example, CH_3 - and CF_3 -terminated SAMs, where the droplets remain stuck, turned out to be ideal for single-crystal growth within each droplet (Figure 2c–f). The average edge dimensions of the single crystals grown within the droplets placed on the ODT and PFDT SAMs were 1.4 ± 0.3 and $0.9 \pm 0.2 \mu\text{m}$, respectively. As previously observed, identical droplets placed on NH_2 -terminated SAMs tended to spread out, resulting in a higher nucleation density and the formation of multiple smaller crystals (edge dimensions 100–400 nm) within each droplet (Figure 2a,b).

To provide further evidence of the formation of HKUST-1 crystals on surfaces using this direct-write pen-type lithographic approach, we first fabricated a 150×150 HKUST-1 array consisting of dots spaced $8 \mu\text{m}$ apart (total area = 1.2 mm^2) on NH_2 - and CF_3 -terminated SAM-modified gold substrates (Figure 3a and Figures S4 and S5) and characterized the dots using XRD. The XRD data shown in Figure 3b clearly demonstrate not only the formation of HKUST-1 crystals but also a crystal growth orientation preference along the $[111]$ direction for both the NH_2 - and CF_3 -terminated SAMs. It is interesting to

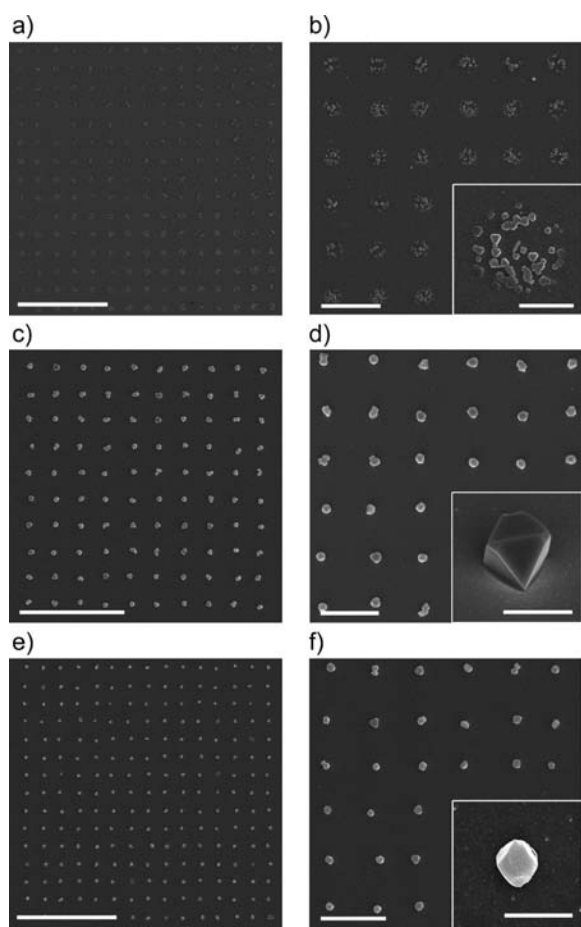


Figure 2. FESEM images of the HKUST-1 arrays fabricated on (a, b) NH_2 -, (c, d) CH_3 -, and (e, f) CF_3 -terminated SAMs on gold substrates. Scale bars represent (a, c, e) $40 \mu\text{m}$, (b, d, f) $10 \mu\text{m}$, and (insets) $2 \mu\text{m}$.

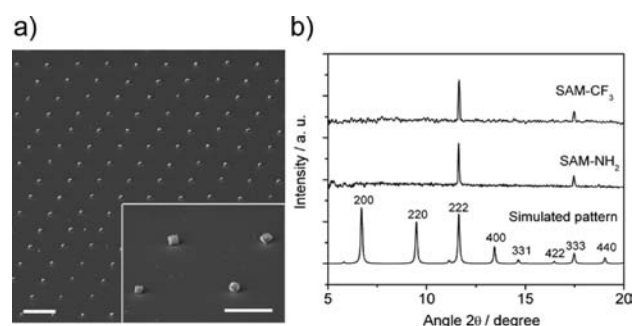


Figure 3. (a) SEM images of a large HKUST-1 array (1.2 mm^2) fabricated on CF_3 -terminated SAMs on gold substrates. Scale bars represent 10 and $4 \mu\text{m}$ for the main and inset images, respectively. (b) XRD patterns (background-corrected) for the HKUST-1 arrays fabricated on the CF_3 - and NH_2 -terminated SAMs, compared with a simulated XRD pattern for HKUST-1.

note that Wöll and co-workers⁷ and Bein and co-workers¹⁶ also observed an identical orientation preference in their crystallization methodologies on OH - and COOH -terminated SAMs, respectively. However, the same authors did not observe crystal growth orientation on hydrophobic SAMs,¹⁴ which was in fact achieved in the HKUST-1 arrays fabricated by the pen-type lithographic technique, as further confirmed by the SEM images (Figure 3a inset).

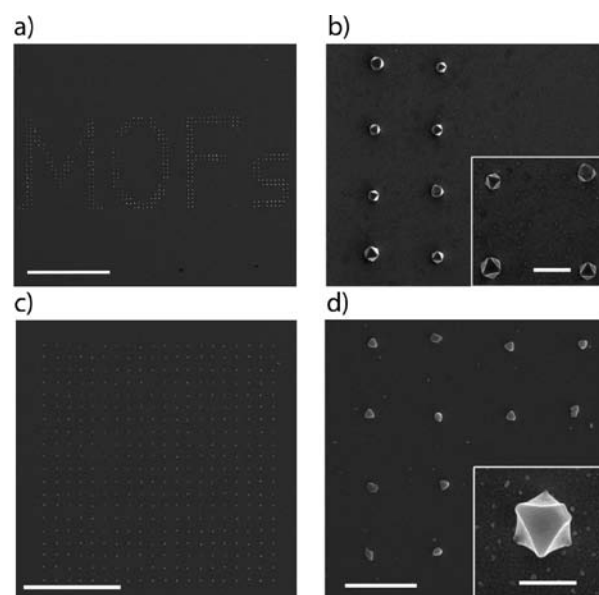


Figure 4. FESEM images of HKUST-1 arrays fabricated on CH_3 -terminated SAMs on gold substrates. (a) The word “MOFs” fabricated with HKUST-1 single crystals and (b) a magnification image of the letter “M”. (c, d) Single-crystal HKUST-1 array composed of crystals with edge dimensions of $550 \pm 100 \text{ nm}$. Scale bars represent (a) $100 \mu\text{m}$, (inset of b) $2 \mu\text{m}$, (c) $40 \mu\text{m}$, (d) $5 \mu\text{m}$, and (inset of d) 500 nm .

Miniaturization of the delivered droplets was also essential for the formation of pure HKUST-1 crystals. Consistent with this conclusion, in control experiments, a mixture of H_3btc , $\text{Cu}(\text{NO}_3)_2 \cdot 2.5\text{H}_2\text{O}$, and nonoriented HKUST-1 crystals was obtained from the evaporation of large DMSO precursor droplets (droplet diameter $\approx 1 \text{ mm}$) on CF_3 -terminated SAMs, as confirmed by optical microscopy, FESEM, and powder XRD (see Figure S6).

This fabrication methodology can also be used to precisely control the location at which a single MOF crystal is grown. For example, 400 single crystals of HKUST-1 were grown on a CH_3 -terminated SAM in such a way that the word “MOFs” was formed (Figure 4a,b). In addition, for a certain dwell time, it is well-known that the time plasma treatment of the SPT strongly influences the volume of the droplet placed on a surface. For longer treatments, the surface of the SPT turns more polar, allowing polar liquids to flow better through the microchannels and consequently resulting in the deposition of larger volumes of liquid. On the contrary, when this time treatment is shorter, the volume of the droplet deposited can be reduced. Following this strategy, we fabricated a 20×20 single-crystal HKUST-1 array on an ODT SAM using an SPT treated with plasma for 30 s instead of 15 min. As Figure 4c,d shows, the single HKUST-1 crystals grown within each droplet were smaller, showing an average edge dimension of $550 \pm 100 \text{ nm}$.

In summary, we have reported a novel, versatile pen-type lithography-based approach for growing HKUST-1 crystals on supports and shown that through the use of surfaces with low wettability it is possible to control the growth of a submicrometer single crystal at a desired location on a surface. Since many functional MOFs have been synthesized, it is likely that this approach can be generalized for controlling the growth of many MOFs at the single-crystal level on several surfaces (see Figure S7). Such capabilities will expand the scope of application for

MOFs in sensors, magnetic and electronic devices, etc., where such control opens new opportunities to integrate them in specific locations of devices. In addition, with our results, one can start to conceive of the generation of combinatorial MOF arrays through delivery of droplets that differ in composition, pH, etc. Once achieved, such parallel fabrication would provide the advantages, for example, of larger libraries for screening the synthesis of novel MOFs.

■ ASSOCIATED CONTENT

S Supporting Information. Experimental details and EDX and FESEM images of HKUST-1 arrays on different surfaces. This material is available free of charge via the Internet at <http://pubs.acs.org>.

■ AUTHOR INFORMATION

Corresponding Author

daniel.maspoch.icn@uab.es

■ ACKNOWLEDGMENT

This work was supported by Projects VALTEC08-2-0003. D.M. and I.I. thank the MICINN for RyC Contracts. C.C. thanks the ICN for a research contract. The authors thank the Servei de Microscopia of the PCB and UAB as well as Pablo García for XRD measurements. We also acknowledge Prof. Laura M. Lechuga for the use of Nano eNabler system.

■ REFERENCES

- (1) (a) Kitagawa, S.; Kitaura, R.; Noro, S. i. *Angew. Chem., Int. Ed.* **2004**, *43*, 2334–2375. (b) Férey, G. *Chem. Soc. Rev.* **2008**, *37*, 191–214. (c) Rosi, N. L.; Eddaoudi, M.; Vodak, D. T.; Eckert, J.; O’Keeffe, M.; Yaghi, O. M. *Science* **2003**, *300*, 1127–1129. (d) Czaja, A. U.; Trukhan, N.; Muller, U. *Chem. Soc. Rev.* **2009**, *38*, 1284–1293. (e) Maspoch, D.; Ruiz-Molina, D.; Veciana, J. *Chem. Soc. Rev.* **2007**, *36*, 770–818.
- (2) (a) Spokoyny, A. M.; Kim, D.; Sumrein, A.; Mirkin, C. A. *Chem. Soc. Rev.* **2009**, *38*, 1218–1227. (b) Lin, W.; Rieter, W.; Taylor, K. *Angew. Chem., Int. Ed.* **2009**, *48*, 650–658. (c) Carné, A.; Carbonell, C.; Imaz, I.; Maspoch, D. *Chem. Soc. Rev.* **2010**, *40*, 291–305.
- (3) (a) Zacher, D.; Shekhah, O.; Wöll, C.; Fischer, R. A. *Chem. Soc. Rev.* **2009**, *38*, 1418–1429. (b) Zacher, D.; Baunemann, A.; Hermes, S.; Fischer, R. A. *J. Mater. Chem.* **2007**, *17*, 2785–2792.
- (4) (a) Allendorf, M. D.; Houk, R. J. T.; Andruskiewicz, L.; Talin, A.; Pikarsky, J.; Chouhury, A.; Gall, K. A.; Hesketh, P. J. *J. Am. Chem. Soc.* **2008**, *130*, 14404–14405. (b) Li, S.-S.; Bux, H.; Feldhoff, A.; Li, G.-L.; Yang, W.-S.; Caro, J. *Adv. Mater.* **2010**, *22*, 3322–3326. (c) Biemmi, E.; Darga, A.; Stock, N.; Bein, T. *Microporous Mesoporous Mater.* **2008**, *114*, 380–386. (d) Lu, G.; Hupp, J. T. *J. Am. Chem. Soc.* **2010**, *132*, 7832–7833. (e) Cobo, S.; Molnar, G.; Real, J.-A.; Bousseksou, A. *Angew. Chem., Int. Ed.* **2006**, *45*, 5786–5789.
- (5) (a) Fan, S.; Chapline, M. G.; Franklin, N. R.; Tomblor, T. W.; Cassell, A. M.; Dai, H. *Science* **1999**, *283*, 512–514. (b) Chen, C. S.; Mrkisch, M.; Huang, S.; Whitesides, G. M.; Ingber, D. E. *Science* **1997**, *276*, 1425–1428. (c) Siringhaus, H.; Kawase, T.; Friend, R. H.; Shimoda, T.; Inbasekaran, M.; Wu, W.; Woo, E. P. *Science* **2000**, *290*, 2123–2126. (d) Huang, Y.; Duan, X.; Wei, Q.; Lieber, C. M. *Science* **2001**, *291*, 630–633. (e) Kasemo, B. *Curr. Opin. Solid State Mater. Sci.* **1998**, *3*, 451–459.
- (6) Hermes, S.; Schröder, F.; Chelmoski, R.; Wöll, C.; Fischer, R. A. *J. Am. Chem. Soc.* **2005**, *127*, 13744–13745.
- (7) Shekhah, O.; Wang, H.; Zacher, D.; Fischer, R.; Wöll, C. *Angew. Chem., Int. Ed.* **2009**, *48*, 5038–5041.

(8) Shekhah, O.; Wang, H.; Paradinas, M.; Ocal, C.; Schupbach, B.; Terfort, A.; Zacher, D.; Fischer, R. A.; Wöll, C. *Nat. Mater.* **2009**, *8*, 481–484.

(9) Li, Y. S.; Liang, F. Y.; Bux, H.; Feldhoff, A.; Yang, W. S.; Caro, J. *Angew. Chem., Int. Ed.* **2010**, *49*, 548–551.

(10) Shekhah, C.; Wang, H.; Kowarik, S.; Schreiber, F.; Paulus, M.; Tolan, M.; Sternemann, C.; Evers, F.; Zacher, D.; Fischer, R. A.; Wöll, C. *J. Am. Chem. Soc.* **2007**, *129*, 15118–15119.

(11) Ameloot, R.; Gobechiya, E.; Uji-i, H.; Martens, J. A.; Hofkens, J.; Alaerts, L.; Sels, B. F.; De Vos, D. E. *Adv. Mater.* **2010**, *22*, 2685–2688.

(12) Vengasandra, S. G.; Lynch, M.; Xu, J.; Henderson, E. *Nanotechnology* **2005**, *16*, 2052–2055.

(13) Piner, R. D.; Zhu, J.; Xu, F.; Hong, S.; Mirkin, C. A. *Science* **1999**, *283*, 661–663.

(14) Reese, M. O.; van Dam, R. M.; Scherer, A.; Quake, S. R. *Genome Res.* **2003**, *13*, 2348–2352.

(15) Chui, S. S.-Y.; Lo, S. M.-F.; Charmant, J. P. H.; Orpen, A. G.; Williams, I. D. *Science* **1999**, *283*, 1148–1150.

(16) Biemi, E.; Scherb, C.; Bein, T. *J. Am. Chem. Soc.* **2007**, *129*, 8054–8055.